Gas-Phase Base-Induced 1,4-Eliminations: Occurrence of Single-, Double-, and Triple-Well E1cb Mechanisms

F. Matthias Bickelhaupt,*,† Godfried J. H. Buisman,‡ Leo J. de Koning,‡ Nico M. M. Nibbering,*,‡ and Evert Jan Baerends§

Contribution from the Computer-Chemie-Centrum, Universität Erlangen-Nürnberg, Nägelsbachstrasse 25, D-91052 Erlangen, Germany, Instituut voor Massaspectrometrie, Universiteit van Amsterdam, Nieuwe Achtergracht 129, NL-1018 WS Amsterdam, The Netherlands, and Afdeling Theoretische Chemie, Scheikundig Laboratorium der Vrije Universiteit, De Boelelaan 1083, NL-1081 HV Amsterdam, The Netherlands

Received February 3, 1995⊗

Abstract: The reactions of the allylic ethers CH_3-CH=CH-CH_2-OEt (**1**), CH_3-CH=CH-CH_2-OMe (**2**), and CH_2=CH-CH_2-OEt (**3**) with a variety of anionic first-row (carbon, nitrogen, oxygen, and fluorine) bases have been investigated with use of FT-ICR mass spectrometry and density-functional theory (DFT). Base-induced 1,4-elimination is an extremely facile process which competes effectively with simple proton transfer 1,2-elimination, and vinylic 1,2-elimination as well as aliphatic (S_N2) and allylic (S_N2') substitution. Overall bimolecular rate constants for base-induced reactions of **1** range from 6×10^{-10} ($F^- + \mathbf{1}$) to 66×10^{-10} ($OH^- + \mathbf{1}$) cm^3 molecule^{-1} s^{-1}. Oxygen bases are the most reactive amongst the employed bases. The ionic products of base-induced 1,4-elimination are either the bare leaving group, RO^-, or the leaving group solvated by the conjugate acid of the base, [BH, RO^-]. The former reaction channel prevails for strong bases (e.g., NH_2^-). The latter pathway becomes dominant for weaker bases (e.g., F^-), because the complexation energy compensates for the reduced exothermicity. This makes the reaction an efficient tool for the preparation of solvated anions under low-pressure conditions. The stereochemistry (i.e., *E* or *Z*) around the β,γ-double bond of the substrate has no detectable influence on the course of base-induced 1,4-eliminations. Deuterium labeling experiments with **2** reveal δ-proton transfer only. The absence of product ions from α-proton transfer is ascribed to a facile electron detachment from the α-allyl anions. The base-induced 1,4-eliminations studied proceed via an E1cb mechanism, as indicated by experiment and shown by theory. This mechanism exists in various modifications amongst which are single-, double-, and triple-well E1cb elimination. To our knowledge, the single-well E1cb mechanism is conceptually unprecedented.

1. Introduction

Base-induced 1,2-eliminations (1,2-E, eq 1a) constitute one of the fundamental types of chemical reactions and are of considerable importance in organic synthesis.[1] They have been thoroughly investigated in condensed[2–5] and gas-phase[6–9] experiments as well as in theoretical studies.[10] Principally, base-induced eliminations are always in competition with another basic reaction type, namely nucleophilic substitution (S_N2, eq1b). Both pathways obey the same mechanistic principles in either the condensed or the gas phase, but the influence of solvation is tremendous. The gas-phase competition between 1,2-E and S_N2 is in general strongly in favor of elimination, whereas nucleophilic substitution prevails in the condensed phase.

† Universität Erlangen-Nürnberg.
‡ Universiteit van Amsterdam.
§ Scheikundig Laboratorium der Vrije Universiteit.
⊗ Abstract published in *Advance ACS Abstracts,* September 15, 1995.

(1) (a) Lowry, T. H.; Richardson, K. S. *Mechanism and Theory in Organic Chemistry*, 2nd ed.; Harper and Row: New York, 1981. (b) Carey, F. A.; Sundberg, R. J. *Advanced Organic Chemistry*, Part A; Plenum Press: New York, 1984. (c) March, J. *Advanced Organic Chemistry*, 4th ed.; Wiley-Interscience: New York, 1992. (d) Reichardt, C. *Solvents and Solvent Effects in Organic Chemistry*, 2nd ed.; VCH Verlags Gesellschaft: Weinheim, 1988.

(2) (a) Gandler, J. R. in *The Chemistry of Double-Bonded Functional Groups*, Vol. 2, Part I; Patai, S. Ed.; Wiley: New York, 1989. (b) Bartsch, R. A.; Závada, J. *Chem. Rev.* **1980**, *80*, 453. (c) Baciocchi, E. *Acc. Chem. Res.* **1979**, *12*, 430. (d) Saunders, W. H., Jr. *Acc. Chem. Res.* **1976**, *9*, 19. (e) Bartsch, R. A. *Acc. Chem. Res.* **1975**, *8*, 239. (f) Bunnett, J. F. *Angew. Chem.* **1962**, *74*, 731. (g) Cram, D. J.; Greene, F. D.; DePuy, C. H. *J. Am. Chem. Soc.* **1956**, *78*, 790. (h) McLennan, D. J. *Tetrahedron* **1975**, *31*, 2999. (i) Biale, G.; Cook, D.; Lloyd, D. J.; Parker, A. J.; Stevens, I. D. R.; Takahashi, J.; Winstein, S. *J. Am. Chem. Soc.* **1971**, *93*, 4735. (j) Parker, A. J.; Ruane, M.; Biale, G.; Winstein, S. *Tetrahedron Lett.* **1968**, 2113.

(3) Hoffman, R. V.; Bartsch, R. A.; Cho, B. R. *Acc. Chem. Res.* **1989**, *22*, 211, and references cited therein.

(4) (a) Eubanks, J. R. I.; Sims, L. B.; Fry, A. *J. Am. Chem. Soc.* **1991**, *113*, 8821. (b) Banait, N. S.; Jencks, W. P. *J. Am. Chem. Soc.* **1990**, *112*, 6950. (c) Gandler, J. R.; Storer, J. W.; Ohlberg, D. A. A. *J. Am. Chem. Soc.* **1990**, *112*, 7756. (d) Bunting, J. W.; Toth, A.; Heo, C. K. M.; Moors, R. G. *J. Am. Chem. Soc.* **1990**, *112*, 8878.

(5) (a) Ölwegård, M.; McEwen, I.; Thibblin, A.; Ahlberg, P. *J. Am. Chem. Soc.* **1985**, *107*, 7494. (b) Thibblin, A.; Sidhu, H. *J. Am. Chem. Soc.* **1992**, *114*, 7403. (c) Thibblin, A. *J. Phys. Org. Chem.* **1992**, *5*, 367.

(6) (a) Bickelhaupt, F. M. *Recl. Trav. Chim. Pays-Bas* **1993**, *112*, 469. (b) Bickelhaupt, F. M.; de Koning, L. J.; Nibbering, N. M. M. *Tetrahedron* **1993**, *49*, 2077. (c) Bickelhaupt, F. M.; de Koning, L. J.; Nibbering, N. M. M. *J. Org. Chem.* **1993**, *58*, 2436. (d) de Koning, L. J.; Nibbering, N. M. M. *J. Am. Chem. Soc.* **1988**, *110*, 2066. (e) van Berkel, W. W.; de Koning, L. J.; Nibbering, N. M. M. *J. Am. Chem. Soc.* **1987**, *109*, 7602. (f) de Koning, L. J.; Nibbering, N. M. M. *J. Am. Chem. Soc.* **1987**, *109*, 1715.

(7) (a) Lum, R. C.; Grabowski, J. J. *J. Am. Chem. Soc.* **1992**, *114*, 9663. (b) Grabowski, J. J.; Lum, R. C. *J. Am. Chem. Soc.* **1990**, *112*, 607. (c) Grabowski, J. J.; Zhang, L. *J. Am. Chem. Soc.* **1989**, *111*, 1193. (d) Lum, R. C.; Grabowski, J. J. *J. Am. Chem. Soc.* **1988**, *110*, 8568.

(8) (a) DePuy, C. H.; Gronert, S.; Mullin, A.; Bierbaum, V. M. *J. Am. Chem. Soc.* **1990**, *112*, 8650. (b) Bierbaum, V. M.; Filley, J.; DePuy, C. H.; Jarrold, M. F.; Bowers, M. T. *J. Am. Chem. Soc.* **1985**, *107*, 2818. (c) DePuy, C. H.; Beedle, E. C.; Bierbaum, V. M. *J. Am. Chem. Soc.* **1982**, *104*, 6483. (d) DePuy, C. H.; Bierbaum, V. M. *J. Am. Chem. Soc.* **1981**, *103*, 5034.

(9) (a) Rabasco, J. J.; Gronert, S.; Kass, S. R. *J. Am. Chem. Soc.* **1994**, *116*, 3133. (b) Haib, J.; Stahl, D. *Org. Mass Spectrom.* **1992**, *27*, 377. (c) Thomas, D. A.; Bloor, J. E.; Bartmess, J. E. *J. Am. Soc. Mass Spectrom.* **1990**, *1*, 295. (d) Kiplinger, J. P.; Tollens, F. R.; Marshall, A. G.; Kobayashi, T.; Lagerwall, D. R.; Paquette, L. A.; Bartmess, J. E. *J. Am. Chem. Soc.* **1989**, *111*, 6914. (e) Jones, M. E.; Ellison, G. B. *J. Am. Chem. Soc.* **1989**, *111*, 1645. (f) van Doorn, R.; Jennings, K. R. *Org. Mass Spectrom.* **1981**, *16*, 397. (g) Ridge, D. P.; Beauchamp, J. L. *J. Am. Chem. Soc.* **1974**, *96*, 637.

0002-7863/95/1517-9889$09.00/0

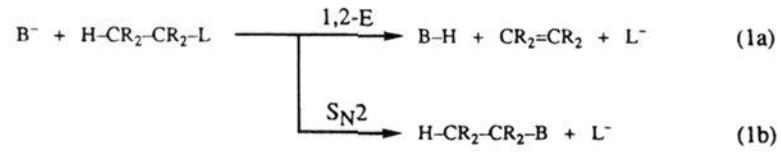

The nature of base-induced 1,2-elimination reactions is now well understood and interpreted in terms of a variable transition state (VTS).[1,2] According to this concept, reactions are categorized according to the geometry of the transition state (TS), which is conceived as being located at one point in a continuous spectrum of mechanistic possibilities. The VTS theory comprises the Bunnet–Cram E2H-spectrum,[2f,g] i.e., E1cb, central E2, and E1 eliminations involving linear proton transfer as well as the Winstein–Parker E2H-E2C-spectrum[2h–j] in which bent proton transfer may occur with a certain degree of base/C^{α} covalent interaction. Recently, we have pointed out that the relative importance of the E2 and S_N2 mechanisms depends directly on the character of the substrate LUMO and that a gradual improvement of the leaving group ability favors substitution.[10a] This constitutes an E2-S_N2 spectrum which builds a bridge between these fundamental mechanisms and helps to understand their mutual competition. Furthermore, stereoelectronic arguments account for the preference of TS structures in which the base and the leaving group are anti- or syn-*periplanar*.[10] The intrinsic preference for base-induced *anti*-elimination has been traced back to the lower energy of the substrate LUMO in the anti-E2 transition state which results in a stronger, more stabilizing interaction with the base HOMO.[10a]

Base-induced 1,4-eliminations (1,4-E eq 2a) have received much less attention.[11–16] Nevertheless, they have important applications in synthetic organic chemistry[13] and play a key role in certain biological processes.[14] Mechanistic studies in the condensed phase have shown that *syn*-1,4-elimination is often but not[11d] always the preferred stereochemical course.[11] Furthermore, base-induced 1,4-elimination can be in competition with 1,2-elimination[11h,m] as well as S_N2 and S_N2' substitution (eq 2b).[12]

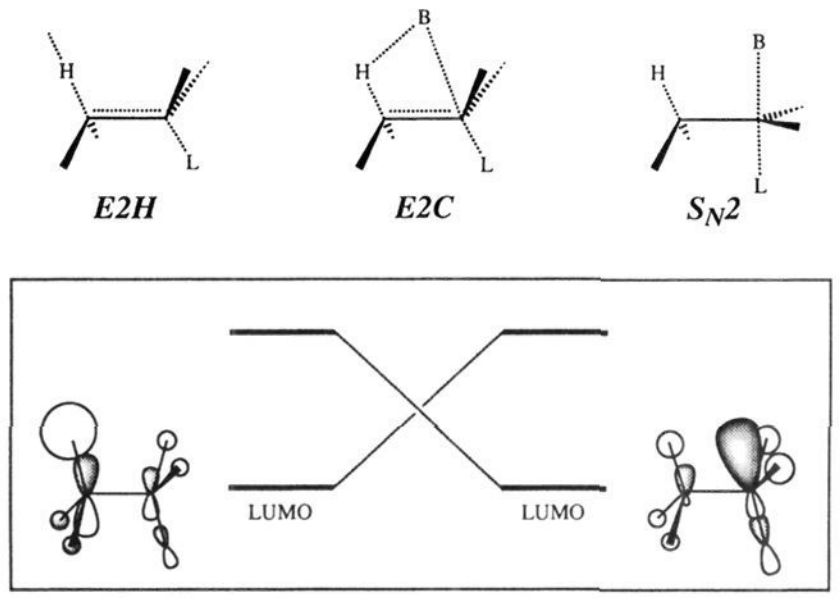

Figure 1. E2-S_N2 spectrum and its relation to the substrate electronic structure.

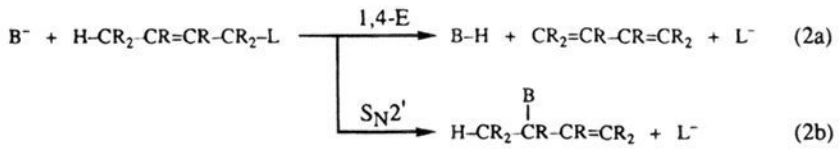

Recently, Rabasco and Kass[15] have investigated the gas-phase base-induced 1,4-eliminations of various differently substituted 1-methoxy-2-cyclohexene substrates (e.g. **A**, eq 3), using flowing afterglow (FA) mass spectrometry. The reactions of $\mathbf{A} + B^-$ appear to afford three product ions: cyclohexadienide (eq 3a), [BH, MeO^-] (eq 3b), and MeO^- (eq 3c). The former two species must result from an elimination, whereas the last might also be formed via substitution. Through specific deuterium labeling of **A** at C^4 or C^6, it was shown that 1,4-elimination dominates for strong bases, whereas 1,2-elimination starts to compete successfully for weaker bases.[15c] This order is reversed, however, after allylic activation of the 1,2-E pathway.[15b] Furthermore, it has been established that *syn*-1,4-elimination is the preferred stereochemical pathway,[15a] in line with early theoretical predictions.[16]

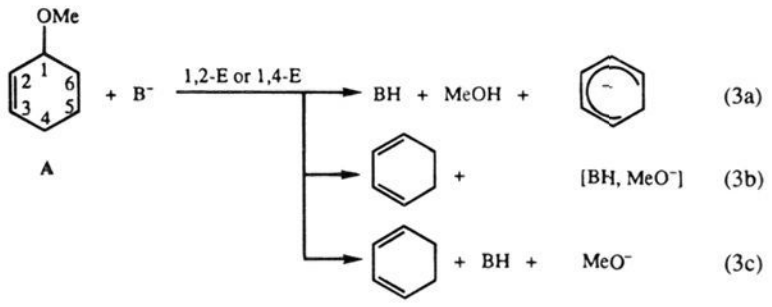

Base-induced 1,4-eliminations still possess a number of incompletely understood aspects. Do they proceed in a one-step E2 or two-step E1cb fashion? What is the effect of the stereochemistry, i.e., *E* or *Z*, around the β,γ-double bond of the substrate?[17] How do base-induced 1,4-eliminations (1,4-E) perform in comparison with other mechanisms, e.g., proton transfer (PT), 1,2-elimination (1,2-E), and vinylic 1,2-elimination ($1,2\text{-}E^{vin}$) as well as aliphatic (S_N2) and allylic (S_N2') nucleophilic substitution?

The purpose of the present paper is to try to answer these and other questions and to better understand the nature of (gas-phase) base-induced 1,4-eliminations. To this end, we have investigated the base-induced reactions of the allylic ethers **1**–**3** (Scheme 1), under the low-pressure conditions of a Fourier

(10) (a) Bickelhaupt, F. M.; Nibbering, N. M. M.; Baerends, E. J.; Ziegler, T. *J. Am. Chem. Soc.* **1993**, *115*, 9160, and references cited therein. (b) Gronert, S. *J. Am. Chem. Soc.* **1993**, *115*, 652. (c) Gronert, S. *J. Am. Chem. Soc.* **1992**, *114*, 2349. (d) Gronert, S. *J. Am. Chem. Soc.* **1991**, *113*, 6041. (e) Dewar, M. J. S.; Yuan, Y.-C. *J. Am. Chem. Soc.* **1990**, *112*, 2088. (f) Dewar, M. J. S.; Yuan, Y.-C. *J. Am. Chem. Soc.* **1990**, *112*, 2095. (g) Minato, T.; Yamabe, S. *J. Am. Chem. Soc.* **1988**, *110*, 4586. (h) Minato, T.; Yamabe, S. *J. Am. Chem. Soc.* **1985**, *107*, 4621.

(11) (a) Ölwegård, M.; Ahlberg, P. *Acta Chem. Scand.* **1990**, *44*, 642. (b) Margot, C.; Matsuda, H.; Schlosser, M. *Tetrahedron* **1990**, *46*, 2425. (c) Fleming, I.; Morgan, I. T.; Sarkar, A. K. *J. Chem. Soc., Chem. Commun.* **1990**, 1575. (d) Ölwegård, M.; Ahlberg, P. *J. Chem. Soc., Chem. Commun.* **1989**, 1279. (e) Tobia, D.; Rickborn, B. *J. Org. Chem.* **1986**, *51*, 3849. (f) Moss, R. J.; Rickborn, B. *J. Org. Chem.* **1986**, *51*, 1992. (g) Hill, R. K.; Bock, M. G. *J. Am. Chem. Soc.* **1978**, *100*, 637. (h) Wenzinger, G. R.; Williams, J. A. *Tetrahedron Lett.* **1973**, 2167. (i) Thummel, R. P.; Rickborn, B. *J. Org. Chem.* **1972**, *51*, 4250. (j) Cristol, S. J. *Acc. Chem. Res.* **1971**, *4*, 393. (k) de la Mare, B. P. D.; Koenigsberger, R.; Lomas, J. S. *J. Chem. Soc. (B)* **1966**, 834. (l) Cristol, S. J.; Barasch, W.; Tieman, C. H. *J. Am. Chem. Soc.* **1955**, *77*, 583. (m) Orloff, H. D.; Kolka, A. J. *J. Am. Chem. Soc.* **1954**, *76*, 5484.

(12) (a) Marshall, J. A.; Blough, B. E. *J. Org. Chem.* **1991**, *56*, 2225. (b) Marshall, J. A. *Chem. Rev.* **1989**, *89*, 1503.

(13) (a) Banwell, M. G.; Halton, B.; Hambley, T. W.; Ireland, N. K.; Papamihail, C.; Russel, S. G. G.; Snow, M. R. *J. Chem. Soc. Perkin Trans. 1* **1992**, 715. (b) Bickelhaupt, F. *Pure Appl. Chem.* **1990**, *62*, 373. (c) Sellén, M.; Bäckvall, J. E.; Hellquist, P. *J. Org. Chem.* **1991**, *56*, 835. (d) Moss, R. J.; White, R. O.; Rickborn, B. *J. Org. Chem.* **1985**, *50*, 5132. (e) Kirby, G. W.; McGuigan, H.; Tan, S. L.; Uff, B. C. *J. Chem. Research (S)* **1985**, 273. (f) Åkermark, B.; Nyström, J.-E.; Rein, T.; Bäckvall, J.-E.; Helquist, P.; Aslanian, R. *Tetrahedron Lett.* **1985**, *25*, 5719. (g) Breitholle, E. G.; Stammer, C. H. *J. Org. Chem.* **1974**, *39*, 1311. (h) Everhardus, R. H.; Peterse, A.; Vermeer, P.; Brandsma, L.; Arens, J. F. *Recl. Trav. Chim. Pays-Bas* **1974**, *93*, 90. (i) Park, J. D.; McMurtry, R. J. *J. Org. Chem.* **1967**, *32*, 2397.

(14) Gerlt, J. A.; Gassman, P. G. *J. Am. Chem. Soc.* **1992**, *114*, 5928.

(15) (a) Rabasco, J. J.; Kass, S. R. *J. Org. Chem.* **1993**, *58*, 2633. (b) Rabasco, J. J.; Kass, S. R. *Tetrahedron Lett.* **1993**, *34*, 765. (c) Rabasco, J. J.; Kass, S. R. *Tetrahedron Lett.* **1991**, *32*, 4077.

(16) (a) Fukui, K.; Fujimoto, H. *Bull. Chem. Soc. Jpn.* **1966**, *39*, 2116. (b) Anh, N. T. *J. Chem. Soc., Chem. Commun.* **1968**, 1089. (c) Tee, O. S.; Altmann, J. A.; Yates, K. *J. Am. Chem. Soc.* **1974**, *96*, 3141.

(17) Vairamani, M.; Saraswathi, M. *Mass Spectrom. Rev.* **1992**, *10*, 491.

Scheme 1

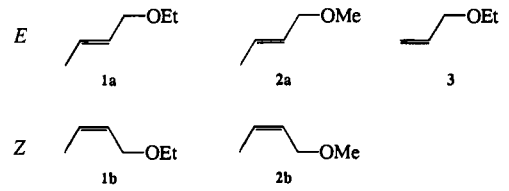

transform ion cyclotron (FT-ICR) mass spectrometer.[18] In particular, we wish to determine the relative contribution of various conceivable mechanisms in 1-ethoxy-2-butene (**1**), which possesses the largest variety of mechanistic possibilities amongst our substrates. The substrates **1**−**3** are designed such that, after combination of all results, the ionic products (which are the only products detected) carry sufficient information to identify the mechanism of their formation (*vide infra*). Furthermore, the scope of base-induced 1,4-eliminations has been explored through a systematic comparison of the reactivity of a variety of first-row (carbon, nitrogen, oxygen, and fluorine) bases. The interpretation of the experimental results is supported by complementary information from density-functional theoretical (DFT) calculations.[19]

2. Methods

A. Experimental Section. General Procedure. The experiments were performed with use of a Fourier transform ion cyclotron resonance (FT-ICR) mass spectrometer constructed at the University of Amsterdam and equipped with a 1.2 T electromagnet and a cubic inch cell. The Segmented Fourier Transform (SEFT) procedure was employed to obtain absolute peak intensities with an accuracy of better than 5%. General operating and experimental procedures have been described previously.[20]

The temperature in the cell was held around 333 K as measured by a thermocouple on the trapping plate opposite the filament. The total pressure in the different experiments was normally kept below 10^{-4} Pa with a background pressure lower than 5×10^{-7} Pa. The pressure was measured with an ionization gauge manometer placed in a side arm of the main pumping line. For the determination of reaction rate constants, the ionization gauge manometer was calibrated for methane by fitting our rate constant for the reaction $CH_4^{\bullet+} + CH_4 \rightarrow CH_5^+ + CH_3^\bullet$ to the average literature value of $(1.11 \pm 0.04) \times 10^{-9}$ cm^3 molecule^{-1} s^{-1}.[21a] Absolute pressures were obtained by correction for the relative sensitivities R_x of the ionization gauge manometer for gases x, using the relationship $R_x = 0.36\alpha + 0.30$ of Bartmess and Georgiadis[21b] and polarizabilities α from Miller.[21c] Overall bimolecular rate constants are accurate to ca. 30% as noted before.[21d]

Ion Generation. NH_2^- was generated via dissociative resonant capture of electrons with a kinetic energy of 5 eV by NH_3. Me_2N^- and $C_6H_5^-$ were produced via proton abstraction from the corresponding conjugate acids by NH_2^-. OH^- was generated via dissociative resonant capture of electrons with a kinetic energy of 6 and 1.5 eV by H_2O (OH^- is formed via proton abstraction from H_2O by initially formed H^-) and N_2O (OH^- is formed via $O^{\bullet-}$ and $H^\bullet$ abstraction from the substrate), respectively. Other anionic oxygen bases were produced either via proton abstraction from the corresponding alcohol by OH^- or via reaction of OH^- with the substrate 1-alkoxy-2-butene. F^- was generated via dissociative resonant capture of electrons with a kinetic energy of 6 eV by CF_4.

Table 1. Bimolecular Overall Rate Constants k (10^{-10} cm^3 molecule^{-1} s^{-1}) and Primary Product Anion Distributions (%) for the Reactions of the Bases B^- with 1-Ethoxy-2-butene (**1**)

B^-	k	$(1\text{-H})^-$	EtO^-	$[BH, EtO^-]$	$C_4H_7O^-$
NH_2^-	41	12	80		8
$C_6H_5^-$	8		100		
Me_2N^-	14	10	89	~1	
OH^-	66		45	42	13
MeO^-	37	~1	17	82	
EtO^- [a]	26			100	
F^-	6			91	9

[a] Both EtO^- and its isolated ^{13}C-component were used.

Chemicals. 1-Ethoxy-2-butenes (**1**) and 1-methoxy-2-butenes (**2**) were prepared by reaction of diethyl and dimethyl sulfate, respectively, with the appropriate (labeled or unlabeled) 2-buten-1-ol.[22a] 2-Buten-1-ol is commercially available as a mixture of *E* and *Z* isomers in a ratio of ca 3:1. *E*-2-Buten-1-ol is obtained from the isomer mixture via preparative GC (column: Reoplex, temperature: 150 °C). *E*-1,1-dideutero-2-buten-1-ol was obtained by reduction of a commercially available *E*-methyl crotonate with lithium aluminum deuteride (LAD).[22b] *Z*-2-buten-1-ol was obtained via (Lindlar) catalytic reduction of commercially available 2-butyn-1-ol with hydrogen.[22c] All other chemicals were commercially available. Purification of all ethers was performed by preparative GC (column: Reoplex, temperature: 60 °C).

B. Theoretical

The quantum chemical calculations were performed at two levels of theory using the Amsterdam-Density-Functional (ADF) program.[23] In all calculations, the MOs were expanded in an uncontracted set of Slater type orbitals (STOs).[23f] The 1s core shells of carbon, nitrogen, oxygen and fluorine were treated by the frozen-core approximation.[23a] An auxiliary set of s, p, d, f, and g STOs was used to fit the molecular density and to represent the Coulomb and exchange potentials accurately in each SCF cycle.[23g] Equilibrium structures were optimized using analytical gradient techniques.[23h] Frequencies were calculated by numerical differentiation of the analytical energy gradients.[23i]

At the lower level, the basis set for H, C, N and O is of double-ζ quality, augmented with one set of polarization functions: 2p on H, 3d on C, N, and O (DZP). For F the basis is of triple-ζ quality, augmented with a 3d and a 4f polarization function (TZ2P). Equilibrium geometries were optimized at the Xα level.[19b] Energies were evaluated using the local density approximation (LDA)[23i] with Becke's nonlocal exchange[23j] and Stoll's correlation[23k] corrections added as perturbation (NL-P).

At the higher level, the basis for *all* atoms is of triple-ζ quality, augmented with two sets of polarization functions on each atom: 2p and 3d on H, 3d and 4f on C, N, O, and F (TZ2P). Equilibrium geometries and energies were evaluated using density-functionals with nonlocal corrections. At the LDA level exchange is described by Slaters

(18) (a) Köster, C.; Kahr, M. S.; Castoro, J. A.; Wilkins, C. L. *Mass Spectrom. Rev.* **1992**, *11*, 495, and references cited therein. (b) Marshall, A. G. *Anal. Chem.* **1991**, *63*, 215A, and references cited therein. (c) Nibbering, N. M. M. *Acc. Chem. Res.* **1990**, *23*, 279. (d) Nibbering, N. M. M. *Adv. Phys. Org. Chem.* **1988**, *24*, 1. (e) Olmstead, W. N.; Brauman, J. I. *J. Am. Chem. Soc.* **1977**, *99*, 4219. (f) Pellerite, M. J.; Brauman, J. I. *J. Am. Chem. Soc.* **1983**, *105*, 2672.

(19) (a) Dreizler, R. M.; Gross, E. K. U. *Density Functional Theory, An Approach to the Quantum Many-Body Problem*; Springer-Verlag: Berlin, 1990. (b) Slater, J. C. *Quantum Theory of Molecules and Solids*, Vol. 4; McGraw-Hill: New York, 1974.

(20) (a) For general operating and experimental procedures, see ref 6f and references cited therein. (b) For the SEFT procedure, see: Koning, L. J. de; Kort, C. W. F.; Pinkse, F. A.; Nibbering, N. M. M. *Int. J. Mass Spectrom. Ion Processes* **1989**, *95*, 71.

(21) (a) Huntress, W. T., Jr.; Laudenslager, J. B.; Pinizzotto, R. F. Jr. *Int. J. Mass Spectrom. Ion Physics* **1974**, *13*, 331. (b) Bartmess, J. E.; Georgiadis, R. M. *Vacuum* **1983**, *33*, 149. (c) Miller, K. J. *J. Am. Chem. Soc.* **1990**, *112*, 8533. (d) van der Wel, H.; Nibbering, N. M. M.; Sheldon, J. C.; Hayes, R. N.; Bowie, J. H. *J. Am. Chem. Soc.* **1987**, *109*, 5823.

(22) (a) Tzeng, D.; Weber, W. P. *J. Org. Chem.* **1981**, *46*, 693. (b) Kingston, D. G. I.; Tannenbaum, H. P. *Org. Mass Spectrom.* **1975**, *10*, 263. (c) Hatch, L. F.; Nesbitt, S. S. *J. Am. Chem. Soc.* **1950**, *72*, 727.

(23) (a) Baerends, E. J.; Ellis, D. E.; Ros, P. *Chem. Phys.* **1973**, *2*, 41. (b) Baerends, E. J.; Ros, P. *Chem. Phys.* **1975**, *8*, 412. (c) Baerends, E. J.; Ros, P. *Int. J. Quantum Chem., Quantum Chem. Symp.* **1978**, *S12*, 169. (d) Boerrigter, P. M.; te Velde, G.; Baerends, E. J. *Int. J. Quantum Chem.* **1988**, *33*, 87. (e) te Velde, G.; Baerends, E. J. *J. Comp. Phys.* **1992**, *99*, 84. (f) Snijders, J. G.; Baerends, E. J.; Vernooijs, P. *At. Nucl. Data Tables* **1982**, *26*, 483. (g) Krijn, J.; Baerends, E. J. Fit-Functions in the HFS-Method, Internal Report (in Dutch), Vrije Universiteit Amsterdam, The Netherlands, 1984. (h) Versluis, L.; Ziegler, T. *J. Chem. Phys.* **1988**, *88*, 322. (i) Vosko, S. H.; Wilk, L.; Nusair, M. *Can. J. Phys.* **1980**, *58*, 1200. (j) Becke, A. D. *J. Chem. Phys.* **1986**, *84*, 4524. (k) Stoll, H.; Golka, E.; Preus, H. *Theoret. Chim. Acta* **1980**, *55*, 29. (l) Fan, L.; Versluis, L.; Ziegler, T.; Baerends, E. J.; Ravenek, W. *Int. J. Quantum Chem., Quantum Chem. Symp.* **1988**, S22, 173. (m) Becke, A. D. *Phys. Rev. A* **1988**, *38*, 3098. (n) Perdew, J. P. *Phys. Rev. B* **1986**, *33*, 8822. Erratum: *Ibid.* **1986**, *34*, 7406. (o) Fan, L.; Ziegler, T. *J. Chem. Phys.* **1991**, *94*, 6057.

Table 2. Proton Affinities PA for the Bases B^- and Reaction Enthalpies ΔH_r (kcal/mol) for the Reactions of B^- with 1-Ethoxy-2-butene (**1**)[a]

B^-	PA	δ-PT	α-PT	1,4-E	1,4-E_{solv}	1,2-E	1,2-E_{solv}	S_N2	S_N2'	1,2-E^{vin}	1,2-E^{vin}_{solv}
NH_2^-	403.7	−26	−19	−15	−25	−13	−23	−26	−26	−3	−13
$C_6H_5^-$	400.8	−23	−16	−12	−22	−10	−20	−35	−33	0	−10
Me_2N^-	396.3	−19	−11	−8	−18	−6	−16	−25	−26	5	−5
OH^-	390.8	−13	−6	−3	−22	0	−19	−11	−11	10	−9
MeO^-	380.5	−3	5	8	−12	10[b]	−9	−6	−6	20	0
EtO^-	377.4	0	8	11	−10	13[b]	−7	−3	−3	24	3
F^-	371.4	6	14	17	−21	10[b]	−16	9	12	30	−8

[a] See section 2.C. [b] 1,3-H-shift/1,2-E: $\Delta H_r = -13$, −10, and −4 kcal/mol for MeO^-, EtO^-, and F^-.

Table 3. Bimolecular Overall Rate Constants k (10^{-10} cm^3 $molecule^{-1}$ s^{-1}) and Primary Product Anion Distributions (%) for the Reactions of the Bases B^- with 1-Methoxy-2-butene (**2**)

B^-	k	(**2**-H)$^-$	MeO^-	[BH, MeO^-]	$C_4H_7O^-$
NH_2^-	43	20	80		
$C_6H_5^-$	6	a	100		
Me_2N^-	b	13	75	12	
OH^-	40	8	38	54	
MeO^- [c]	23	20	18	62	
EtO^-	16			100	
F^-	11			100	

[a] Formation of traces. [b] Not determined. [c] CD_3O^- was used.

Xα potential[19b] and correlation is treated in the Vosko–Wilk–Nusair (VWN) parametrization.[23i] Nonlocal corrections for the exchange due to Becke[23j,23m] and for correlation due to Perdew[23n] are added self-consistently (NL-SCF).[23o]

C. Thermochemistry

Enthalpies of reaction were calculated with data from the literature,[24] our theoretical calculations (Tables 8 and 9), and some estimated quantities.[25] Throughout this work, we adapt the convention that proton affinity (PA) and electron affinity (EA) are defined as the system's enthalpy changes for the reactions $BH \rightarrow B^- + H^+$ and $B^- \rightarrow B^\cdot + e^-$, respectively.[24a] Primarily, the theoretical calculations yield the electronic energy changes at 0 K for deprotonation and vertical electron detachment, i.e., ΔE_{PA} and ΔE_{EA} vert, respectively. Proton affinities for a series of test bases B^- were calculated by adding the 298.15 K thermal energy correction obtained from frequency calculations to the corresponding ΔE_{PA} value (see Table 7). The proton affinities for the vinylic (**2b**-H^β)$^-$ and the allylic (**3**-H^α)$^-$, (**2b**-H^α)$^-$, and (**2b**-H^δ)$^-$ anions were obtained using the thermal energy corrections calculated for $C_2H_3^-$ and $C_3H_5^-$, respectively (see Table 8).

3. Results

The results are summarized in Tables 1–9 and Figures 2 and 3. In the following, we discuss the base-induced reactions of the allylic ethers **1**–**3** (subsection A) and the results of labeling and other complementary FT-ICR experiments (subsection B). Next, the results of the density-functional (DF) theoretical study of the reaction systems OH^- and F^- + **2b** are presented (subsection C). Finally, the combined experimental and theoretical results are evaluated in section 4 (Discussion).

A. Base-Induced Reactions of the Allylic Ethers. The Effect of *E*/*Z* Stereochemistry. First, we wish to clarify the effect of the *E*/*Z* stereochemistry on the reactivity of **1** and **2**, before the individual reactions are considered in more detail. To this end, the pure *E* and *Z* stereoisomers of **1** and **2** (Scheme 1) have been reacted with NH_2^-, $C_6H_5^-$, OH^-, and F^-. The reaction rates and primary product ion distributions of **1a** and **1b**, on the one hand, and of **2a** and **2b**, on the other hand, appear to be equal within the experimental accuracy. We thus conclude that the *E*/*Z* stereochemistry has a negligible effect on the reactivity of **1** and **2**. Therefore, the readily available stereoisomer mixtures of **1** and **2** (*E*:*Z* ≈ 3:1) are employed in all further experiments, unless stated otherwise!

Table 4. Proton Affinities PA for the Bases B^- and Reaction Enthalpies ΔH_r (kcal/mol) for the Reactions of B^- with 1-Methoxy-2-butene (**2**)[a]

B^-	PA	δ-PT	α-PT	1,4-E	1,4-E_{solv}	S_N2	S_N2'	1,2-E^{vin}	1,2-E^{vin}_{solv}
NH_2^-	403.7	−26	−19	−12	−22	−28	−23	0	−10
$C_6H_5^-$	400.8	−23	−16	−9	−19	−39	−29	4	−7
Me_2N^-	396.3	−19	−11	−5	−15	−28	−23	8	−2
OH^-	390.8	−13	−6	1	−23	−11	−8	13	−11
MeO^-	380.5	−3	5	11	−18	−7	−3	23	−5
EtO^-	377.4	0	8	14	−9	−3	0	27	4
F^-	371.4	6	14	20	−19	5	15	33	−6

[a] See section 2.C.

Table 5. Bimolecular Overall Rate Constants k (10^{-10} cm^3 $molecule^{-1}$ s^{-1}) and Primary Product Anion Distributions (%) for the Reactions of the Bases B^- with 1-Ethoxy-2-propene (**3**)

B^-	k	(**3**-H)$^-$	EtO^-	$C_3H_5O^-$	[BH, $C_3H_5O^-$]
NH_2^-	19	44	37	19	
$C_6H_5^-$	2		55	45	
OH^-	34	~1	4	95	
F^-	1			78	22

Table 6. Proton Affinities PA for the Bases B^- and Reaction Enthalpies ΔH_r (kcal/mol) for the Reactions of B^- with 3-Ethoxypropene (**3**)[a]

B^-	PA	α-PT	1,2-E	1,2-E_{solv}	S_N2	S_N2'	1,2-E^{vin}	1,2-E^{vin}_{solv}
NH_2^-	403.7	−18	−15	−25	−28	−27	−4	−14
$C_6H_5^-$	400.8	−15	−12	−22	−37	−29	−1	−11
OH^-	390.8	−5	−2	−21	−13	−9	9	−10
F^-	371.4	14	17[b]	−17	7	11	29	−8

[a] See section 2.C. [b] 1,3-H-shift/1,2-E: $\Delta H_r = -6$ kcal/mol.

Table 7. Calculated[a] and Experimental[b] Proton Affinities (PA) and Electron Affinities (EA) for Selected Anionic Bases (in kcal/mol)

proton affinities	PA (theor)	PA (exp)
CH_3^-	420.2	416.8 ± 2
$C_2H_3^-$	408.1	406.1
NH_2^-	406.4	403.7 ± 0.7
OH^-	394.0	390.8
$CH_2{=}CH{-}CH_2^-$	389.3	390.8 ± 2.4
CH_3O^-	380.9	380.5 ± 2
F^-	376.1	371.4 ± 0.2
electron affinities	**ΔE_{EA}^{vert}(theor)**	**EA (exp)**
$C_2H_3^-$	20.3	18 ± 5
$CH_2{=}CH{-}CH_2^-$	3.3	9.5 ± 3.9

[a] NL-P/DZP//Xα/DZP, for F: TZ2P. PAs include 298.15 K thermal energy correction. [b] Reference 24a.

(24) (a) Lias, S. G.; Bartmess, J. E.; Liebman, J. F.; Holmes, J. L.; Levin, R. D.; Mallard, W. G. *J. Phys. Chem. Ref. Data* **1988**, *17*, Suppl. No. 1. (b) Benson, S. W. *Thermochemical Kinetics*, 2nd ed.; Wiley: New York, 1976. (c) Graul, S. T.; Squires, R. R. *J. Am. Chem. Soc.* **1990**, *112*, 2517.

(25) The following thermochemical quantities were estimated. (a) But-1-enoxide: $\Delta H_f \approx -51$ kcal/mol. (b) [1,3-Butadiene, MeO^-]: $\Delta H_{com} \approx \Delta E_{com}$(Table 9). (c) [1,3-Butadiene, EtO^-]: $\Delta H_{com} \approx \Delta E_{com}$ of [1,3-butadiene, MeO^-] (Table 9). (d) 1-Ethoxy-2-butene (**1**): $PA^{\alpha,\beta,\delta} \approx PA^{\alpha,\beta,\delta}$ of 1-methoxy-2-butene (**2**) (Table 8). (e) [BH, RO^-]: $\Delta H_{com} \approx -10$ kcal/mol (BH=NH_3, C_6H_6, Me_2NH; RO^- = MeO^-, EtO^-, 2-butenoxide, 2-propenoxide), ≈ −19 kcal/mol (BH=H_2O; RO^-=EtO^-, but-2-enoxide, prop-2-enoxide), ≈ −19 kcal/mol (BH=MeOH; RO^-=but-2-enoxide), ≈ −20 kcal/mol (BH=EtOH; RO^-=but-2-enoxide). (f) [B^-, ROH]: $\Delta H_{com} \approx -32$ kcal/mol (B^-=F^-; ROH=but-2-enol, prop-2-enol).

Table 8. Calculated Proton Affinities (PA) and Vertical Electron Detachment Energies ($\Delta E_{EA^{ver}}$) for Selected Anions $(M-H)^-$ (in kcal/mol)[a]

$(M-H)^-$ [b]	PA	$\Delta E_{EA^{ver}}$
$(\mathbf{2b}\text{-}H^{\beta})^-$	394.6	23.2
$(\mathbf{3}\text{-}H^{\alpha})^-$	385.4	3.5
$(\mathbf{2b}\text{-}H^{\alpha})^-$	385.0	0.9
$(\mathbf{2b}\text{-}H^{\delta})^-$	377.6	14.1

[a] NL-P/DZP//Xα/DZP (see also Table 7 and section 2.C). [b] **2b** = Z-1-methoxy-2-butene; **3** = 1-ethoxy-2-propene (Scheme **1**).

Product Ion Distributions and Rate Constants. The reactions of **1**–**3** (Scheme 1) with a number of anionic first-row bases B^- (for **1** and **2**: $B^- = NH_2^-, C_6H_5^-, Me_2N^-, OH^-, MeO^-, EtO^-, F^-$; for **3**: $B^- = NH_2^-, C_6H_5^-, OH^-, F^-$) have been investigated. The results, i.e., bimolecular overall rate constants and primary product ion distributions, are summarized in Tables 1–5. The corresponding thermochemical data are given in Tables 2–6.

The base-induced reactions of CH_3-CH=CH-CH_2-OEt (**1**) lead to the formation of four different product ions, namely $(\mathbf{1}\text{-}H)^-$, EtO^-, [BH, EtO^-], and $C_4H_7O^-$ (Table 1, eq 4). The proton transfer product $(\mathbf{1}\text{-}H)^-$ is observed for NH_2^-, Me_2N^-, and MeO^- where it accounts for 12, 10, and 1% of the product ions formed, respectively. The formation of EtO^- occurs for the bases NH_2^- (80%) through MeO^- (17%). Its formation is gradually taken over by that of the ion/molecule complex [BH, EtO^-] with decreasing proton affinity (PA) of the base. The formation of [BH, EtO^-] begins with the base Me_2N^- and increases rapidly from 1 to more than 90% along the series OH^-, MeO^-, EtO^-, and F^- (Table 1). The product ion $C_4H_7O^-$ is generated in the reactions of **1** with NH_2^- (8%), OH^- (13%), and F^- (9%). Rate constants range from 6×10^{-10} (F^-) via 8×10^{-10} ($C_6H_5^-$) and 41×10^{-10} (NH_2^-) up to 66×10^{-10} (OH^-) cm^3 $molecule^{-1}$ s^{-1}.

$$CH_3\text{-}CH{=}CH\text{-}CH_2\text{-}OEt \xrightarrow{B^-} (1\text{-}H)^- + EtO^- + [BH, EtO^-] + C_4H_7O^- \quad (4a)$$
1

$$\xrightarrow{\times} [BH, C_4H_7O^-] \quad (4b)$$

The base-induced reactions of CH_3-CH=CH-CH_2-OMe (**2**) lead to the formation of three different product ions, namely $(\mathbf{2}\text{-}H)^-$, MeO^-, and [BH, MeO^-] (Table 3, eq 5). The proton transfer product $(\mathbf{2}\text{-}H)^-$ is observed for NH_2^-, $C_6H_5^-$ (traces), Me_2N^-, OH^-, and MeO^- (Table 3); it is generated in much higher relative abundance than $(\mathbf{1}\text{-}H)^-$ in the reactions of **1** (Table 1). The base-induced formation of MeO^- from **2** occurs for the bases NH_2^- (80%) through MeO^- (18%). With decreasing proton affinity (PA) of the base, its formation is gradually taken over by that of the ion/molecule complex [BH, MeO^-], starting with Me_2N^- (12%). This trend parallels the results for **1**. Note, that the base-induced formation of $C_4H_7O^-$ from **2** is not observed. Rate constants for **2** have essentially the same magnitude as those for **1** and range from 6×10^{-10} ($C_6H_5^-$) via 11×10^{-10} (F^-) and 40×10^{-10} (OH^-) up to 43×10^{-10} (NH_2^-) cm^3 $molecule^{-1}$ s^{-1}.

$$CH_3\text{-}CH{=}CH\text{-}CH_2\text{-}OMe \xrightarrow{B^-} (2\text{-}H)^- + MeO^- + [BH, MeO^-] \quad (5a)$$
2

$$\xrightarrow{\times} C_4H_7O^- + [BH, C_4H_7O^-] \quad (5b)$$

The base-induced reactions of CH_2=CH-CH_2-OEt (**3**) lead to the formation of four different product ions, namely $(\mathbf{3}\text{-}H)^-$, EtO^-, $C_3H_5O^-$, and [BH, $C_3H_5O^-$] (Table 5, eq 6). The proton transfer product $(\mathbf{3}\text{-}H)^-$ is observed for NH_2^- (44%) and OH^- (1%). The base-induced formation of EtO^- from **3** occurs for the bases NH_2^- (37%) through OH^- (4%); it is generated in a much lower relative abundance than in the reactions of **1**. Furthermore, the formation of the ion/molecule complex [BH, EtO^-] is not observed, again at variance with the reactions of **1**. The formation of $C_3H_5O^-$ from **3** occurs for all bases (i.e.; NH_2^-, $C_6H_5^-$, OH^-, and F^-) and is dominant for the weaker bases OH^- and F^- (Table 5). The product [BH, $C_3H_5O^-$] is only detected in the reaction of **3** with F^- (22%). Note, that the corresponding ion in the reactions of **1** and **2**, i.e.; [BH, $C_4H_7O^-$], is not observed. Rate constants for **3** are significantly lower than those for **1** and **2**. They range from 1×10^{-10} (F^-) via 2×10^{-10} ($C_6H_5^-$) and 19×10^{-10} (NH_2^-) up to 34×10^{-10} (OH^-) cm^3 $molecule^{-1}$ s^{-1}.

$$CH_2{=}CH\text{-}CH_2\text{-}OEt \xrightarrow{B^-} (3\text{-}H)^- + EtO^- + C_4H_7O^- + [BH, C_4H_7O^-] \quad (6a)$$
3

$$\xrightarrow{\times} [BH, EtO^-] \quad (6b)$$

Identification of Mechanistic Pathways. Next, we consider how the mechanisms that are active in the formation of certain product ions can be identified. The base-induced reactions of 1-ethoxy-2-butene (**1**) may proceed via several *a priori* conceivable mechanistic pathways, as shown in Scheme 2. A problem arises as certain mechanisms cannot be mass spectrometrically distinguished, because they produce ions of equal *m/z* (e.g., EtO^- could be formed via four different pathways, see Scheme 2). This problem is largely solved by studying the base-induced reactions of 1-methoxy-2-butene (**2**) and 1-ethoxy-2-propene (**3**) in which a number of pathways has been principally eliminated (see Scheme 2: "pathways principally available..."). Now, the reduction in the rate of formation of a certain product ion (or its disappearance) can be associated with the eliminated pathway, whereas the eventually remaining formation is due to the still available mechanism. Furthermore, pathways can be excluded if they are significantly more endothermic than 5–10 kcal/mol.[26] In this way, it is possible to estimate the relative contributions of different mechanisms which produce ions of equal *m/z* (still other ways to identify mechanisms are discussed in subsection B).

Formation of $(M-H)^-$. The base-induced formation of $(\mathbf{1}\text{-}H)^-$ and $(\mathbf{2}\text{-}H)^-$ (Tables 1 and 3) conceivably proceeds via α- or δ-proton transfer, for which relatively stable allylic anions are generated (PT, Scheme 2). The combined results of experiments with specifically deuterium labeled **2** (subsection B) and theoretical calculations on the proton affinities (PAs) of various $(\mathbf{2b}\text{-}H)^-$ ions (subsection C) show that δ-PT is the dominant, if not exclusive pathway to the *observed* (*!*) $(\mathbf{1}\text{-}H)^-$ and $(\mathbf{2}\text{-}H)^-$ ions (*vide infra*). The product ion $(\mathbf{3}\text{-}H)^-$ (Table 5) is considered to be the relatively stable allylic anion which is formed via α-PT (no δ-PT is possible).

Formation of EtO^- and MeO^-. The base-induced formation of EtO^- from **1** (Table 1) could in principle be due to allylic (S_N2') and aliphatic ($S_N2@C^{\alpha}$) nucleophilic substitution, vinylic 1,2-elimination (1,2-E^{vin}) and 1,4-elimination (1,4-E, Scheme 2). The $S_N2@C^{\alpha}$ pathway is excluded, because even the sterically less hindered and thus more feasible substitution at $C^{\alpha'}$ ($S_N2@C^{\alpha'}$) is not active. This is concluded from the absence of $C_4H_7O^-$ amongst the product ions in the reactions of **2** (eq 5b), where $S_N2@C^{\alpha'}$ (i.e., S_N2 at CH_3) would have been the only viable route (Scheme 2). The rate constants drop dramatically when going from **1** to **3**, a change which we associate with the removal of the 1,4-E mechanism after replacement of the δ-methyl group by hydrogen. The remaining formation of

(26) In principle, low-pressure reactions must be exothermic or thermoneutral (see refs 18c and 18d). However, reactants may overcome some endothermicity due to their thermal energy plus a few kcal/mol which have been absorbed during the ion isolation procedure.

Scheme 2

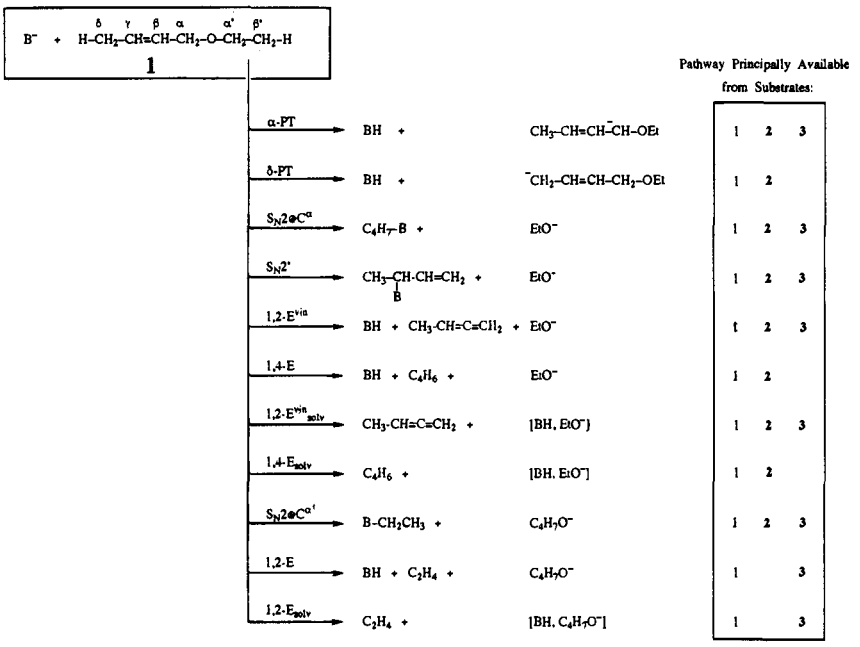

EtO^- (observed for **3** + NH_2^-, $C_6H_5^-$, and OH^-, Table 5) is ascribed to a 1,2-E^{vin} elimination and/or S_N2' substitution. The combined relative contribution 1,2-E^{vin} and S_N2' in the reactions of **1** is now estimated by assuming that they contribute with more or less equal efficiencies in the corresponding base-induced reactions of **1** and **3**. In fact, in this way one obtains upper limits for the contributions of 1,2-E^{vin} + S_N2', because the occurrence of 1,4-elimination in **1** effectively reduces the probability of other mechanisms. Thus, the approximate relative contribution of 1,4-E in the reactions of **1** + NH_2^-, $C_6H_5^-$, OH^-, and F^- is larger than or equal to 63%, 86%, 43% and 0%, respectively, and that of 1,2-E^{vin} + S_N2' is less than 17%, 14%, 2%, and 0%, respectively (using data from Tables 1 and 5). Similarly, the formation of MeO^- in the base-induced reactions of **2** (Table 3) is mainly ascribed to the 1,4-E mechanism.

Formation of [BH, EtO^-] and [BH, MeO^-]. The solvated leaving group [BH, EtO^-], which is observed in the base-induced reactions of **1** (Table 1), could in principle be formed via vinylic 1,2-elimination (1,2-E^{vin}_{solv}) and 1,4-elimination (1,4-E_{solv}, Scheme 2). Its formation vanishes when going from **1** to **3**, a change which we associate with the removal of the 1,4-E_{solv} mechanism after replacement of the δ-methyl group by hydrogen. Thus, [BH, EtO^-] is entirely produced via the 1,4-E_{solv} pathway, whereas the 1,2-E^{vin}_{solv} mechanism has no detectable contribution. Similarly, the formation of [BH, MeO] in the base-induced reactions of **2** (Table 3) is ascribed to the 1,4-E_{solv} pathway. The fraction of the solvated with respect to the free leaving group increases when the proton affinity of the base decreases (Tables 1 and 3). This is explained by the fact that the energy released upon complexation between conjugate acid and leaving group becomes increasingly important to fuel the reaction (Tables 2 and 4).

Formation of $C_4H_7O^-$ and $C_3H_5O^-$. The base-induced formation of $C_4H_7O^-$ from **1** (Table 1) could in principle be due to nucleophilic substitution at $C^{\alpha'}$ ($S_N2@C^{\alpha'}$) and 1,2-elimination (1,2-E, Scheme 2). The $S_N2@C^{\alpha'}$ substitution is excluded, as mentioned before, because no $C_4H_7O^-$ is formed in the reactions of **2** (eq 5b), where it would have been the only viable route (Scheme 2). This leaves the 1,2-elimination, which is a suitable pathway for the NH_2^- and OH^- induced reactions. However, this pathway becomes highly endothermic, i.e., +19 kcal/mol, in the case of the base F^- (Table 2). The same holds for the corresponding formation of $C_3H_5O^-$ from **3**, which is 17 kcal/mol endothermic in the case of F^- (Table 6). Therefore, we propose an alternative mechanism (1,3-H-shift/1,2-E) for the F^- induced formation of $C_4H_7O^-$ from **1** and $C_3H_5O^-$ from **3** (eq 7). First, a base-induced allylic hydrogen rearrangement (1,3-H-shift) takes place in the product complex with the rather unreactive F^- (eq 7). Thus, an intermediate complex with a vinylic ether is generated which, finally, undergoes an F^- induced 1,2-E elimination (eq 7). The F^- induced 1,3-H-shift/1,2-E eliminations of **1** and **3** are exothermic by −4 and −6 kcal/mol, respectively, due to the formation of a relatively stable enolate anion. Finally, in the F^- induced reaction of **3** (Table 5) the solvated leaving group [BH, $C_3H_5O^-$] is formed either via a normal 1,2-elimination (1,2-E_{solv}) or again via a 1,3-H-shift/1,2-E elimination (eq 7) which both are exothermic (Table 6). Summarizing, the formation of $C_4H_7O^-$ in the base-induced reactions of **1** is ascribed either to a straightforward 1,2-E elimination ($B^- = NH_2^-$, OH^-) or to a 1,3-H-shift/1,2-E elimination ($B^- = F^-$).

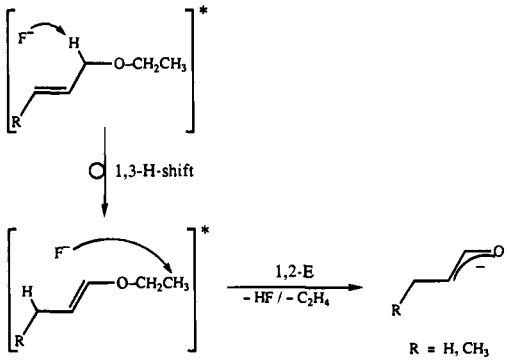

(7)

B. Experimental Investigation of the $(M-H)^-$ Structure. α-PT vs δ-PT. To investigate if $(1-H)^-$ and $(2-H)^-$ are formed via α-proton transfer (α-PT) or δ-proton transfer (δ-PT, Scheme 2), we have studied the reactions of the α-dideuterated 1,1-dideutero-1-methoxy-2-butene (**2a**-*1,1-d*$_2$) with NH_2^-, OH^-, and $C_6H_5^-$ (eq 8). The exclusive formation of $(M-H)^-$, i.e., proton transfer, is observed (eq 8b), besides the generation of MeO^- and, for $B^- = OH^-$, [H_2O, MeO^-] (eq 8a). The formation of $(M-D)^-$, i.e. deuteron transfer, was not detected (eq 8c). We

thus conclude that the base-induced formation of $(2\text{-H})^-$ and, in analogy, $(1\text{-H})^-$ proceeds essentially via δ-PT (this conclusion also holds if one takes an H/D-isotope effect of 2−5 into account).

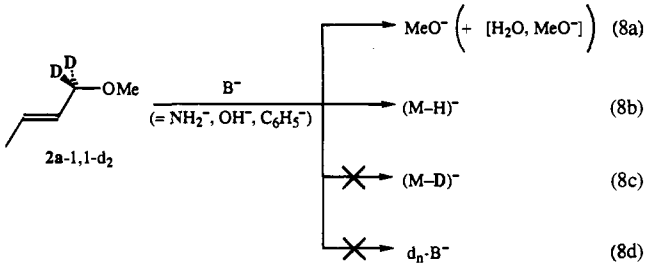

(8a)
(8b)
(8c)
(8d)

The question remains, *why* $(\text{M-H}^\delta)^-$ but no $(\text{M-D}^\alpha)^-$ is observed in the base-induced reactions of **2a**-*1,1-d*$_2$ (eq 8). The NL-P/DZP//Xα/DZP calculations on **2b** show that the δ-hydrogen (ΔH_{acid} = 377.6 kcal/mol) is ca. 7 kcal/mol more acidic than the α-hydrogen (ΔH_{acid} = 385.0 kcal/mol, Table 8). This accounts for a more rapid formation of $(\text{M-H}^\delta)^-$, but the complete absence of $(\text{M-D}^\alpha)^-$ is not satisfactorily explained. A possible explanation could be that $(\text{M-D}^\alpha)^-$ is formed but is subject to facile thermal electron detachment (eq 9). This hypothesis is supported by the calculated vertical electron detachment energy ($\Delta E_{EA^{vert}}$) of $(\mathbf{2b}\text{-H}^\alpha)^-$ which is only 0.9 kcal/mol (Table 8). For comparison, $\Delta E_{EA^{vert}}$ is 14.1 kcal/mol for $(\mathbf{2b}\text{-H}^\delta)^-$ (Table 8). Facile electron detachment from 1-substituted allyl anions has also been invoked to explain signal loss in base-induced reactions of 1-substituted propenes at ambient temperatures in a flowing afterglow (FA) device.[27]

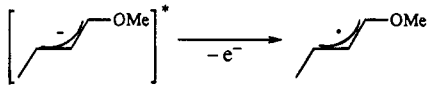

(9)

The nonoccurrence of deuterium incorporation in the bases (eq 8d) indicates, that no α-hydrogen exchange takes place prior to δ-PT. This is confirmed by the absence of deuterium incorporation into $(2\text{-H})^-$ in the reaction of OD^- with **2** (eq 10). This indicates also that the 1,3-H-shift/1,2-E mechanism (as proposed for F^- induced reactions, eq 7) does not contribute to the NH_2^- and OH^- induced formation of $C_4H_7O^-$ from **1** (Table 1).

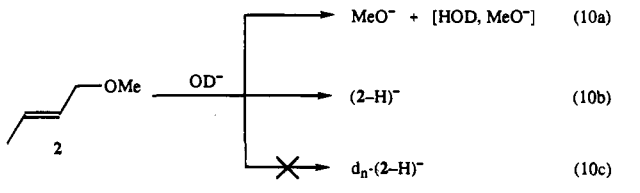

(10a)
(10b)
(10c)

Allyl Anion vs Ion/Molecule Complex. Next, the question is addressed whether the detected $(1\text{-H})^-$ and $(2\text{-H})^-$ ions exist as δ-allyl anions or as an ion/molecule complex $[C_4H_6, RO^-]$. To this end, $(2\text{-H})^-$ is generated from **2** via proton abstraction by amide and allowed to react in the presence of ND_3 + **2** which are at comparable partial pressures (eq 11). This leads to the production of MeO^- (ca. 60%, eq 11a) and $[ND_3, MeO^-]$ (ca. 40%, eq 11b). No deuterium is incorporated into $(2\text{-H})^-$ (eq 11c). The formation of MeO^- must be due to a (slightly endothermic) simple dissociation of $(2\text{-H})^-$. The formation of $[ND_3, MeO^-]$ is ascribed either to ND_3 assisted dissociation of an allylic $(2\text{-H})^-$ structure or to neutral exchange in the $[C_4H_6, MeO^-]$ complex. The fraction of the MeO^- product can be increased to ca. 90%, through specific excitation of the cyclotron

Scheme 3

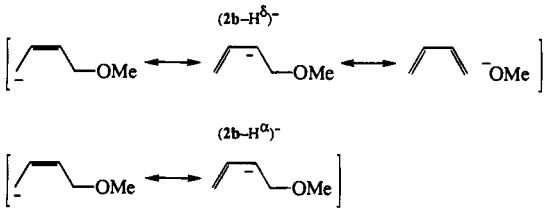

motion of $(2\text{-H})^-$ (eq 11a). These data point to a rather weakly bound $(2\text{-H})^-$ structure.

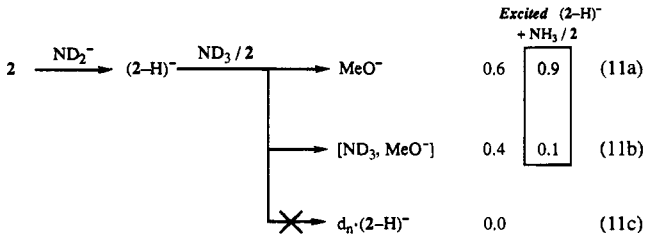

(11a)
(11b)
(11c)

Summarizing, the observed $(\text{M-H})^-$ ions are formed via δ-PT and consist of weakly bound C_4H_6 and RO^- fragments. Further data concerning the $(\text{M-H})^-$ structure are provided by the theoretical calculations (subsection C).

C. Theoretical Results. The proton affinities and vertical electron detachment energies for a number of $(\text{M-H})^-$ ions have been calculated to support the interpretation of the experimental results. Furthermore, the potential energy surfaces for the 1,4-elimination of OH^- and F^- + **2b** have been investigated to strengthen our conception of the mechanism. However, we first take a look at a series of test calculations which probe the accuracy of the calculations.

Accuracy of the DF Calculations. The proton affinities (PA) and vertical electron detachment energies ($\Delta E_{EA^{vert}}$) have been calculated for a series of relevant anions for which experimental data are available (Table 7), to probe the accuracy of the NL-P/DZP//Xα/DZP (for F: NL-P/TZ2P//Xα/TZ2P) density-functional (DF) calculations. The calculated PA values for CH_3^-, $C_2H_3^-$, NH_2^-, OH^-, CH_2=CH-CH_2^-, CH_3O^-, and F^- agree well with the experimental PAs, the maximum deviation being +4.7 kcal/mol for the fluoride anion (Table 7). The calculated $\Delta E_{EA^{vert}}$ values for $C_2H_3^-$ (20.3 kcal/mol) and CH_2=CH-CH_2^- (3.3 kcal/mol) exhibit larger deviations from the experimental EAs of 18 ± 5 and 9.5 ± 3.9 kcal/mol, respectively, but the trend is correctly reproduced. The OH^- and F^- + **2b** potential energy surfaces are also investigated at NL-SCF/TZ2P//NL-SCF/TZ2P. At this higher level, the proton affinities for OH^- and F^- are 395.4 and 376.3 kcal/mol, thus deviating only slightly from the lower level calculations. We conclude that our DF calculations yield accurate PAs, in particular for allyl anion systems, and correct trends for EAs.

PA and $\Delta E_{EA^{vert}}$ Values for $(\text{M-H})^-$ Ions. The PA and $\Delta E_{EA^{vert}}$ values have been calculated for $(\mathbf{2b}\text{-H}^\alpha)^-$, $(\mathbf{2b}\text{-H}^\beta)^-$, $(\mathbf{2b}\text{-H}^\delta)^-$, and $(\mathbf{3}\text{-H}^\alpha)^-$ (Table 8; NL-P/DZP//Xα/DZP). The vinylic $(\mathbf{2b}\text{-H}^\beta)^-$ has the strongest proton affinity (394.6 kcal/mol, Table 8) of the four anions, but it has been substantially stabilized with respect to the prototype $C_2H_3^-$ (408.1 kcal/mol, Table 7). The two allyl anions of **2b** are both 10 or more kcal/mol more stable, i.e., less basic. The $(\mathbf{2b}\text{-H}^\delta)^-$ ion (PA = 377.6 kcal/mol) is even 7.4 kcal/mol more stable than $(\mathbf{2b}\text{-H}^\alpha)^-$ (PA = 385.0 kcal/mol, Table 8). The additional stability of $(\mathbf{2b}\text{-H}^\delta)^-$ can be ascribed to negative hyperconjugation into the C−O bond, which is not possible in $(\mathbf{2b}\text{-H}^\alpha)^-$ (Scheme 3). The vertical electron detachment energies of the allyl anions are considerably lower than those of the vinyl anions (Tables 7 and 8). However, the stability of $(\mathbf{2b}\text{-H}^\delta)^-$ with respect to electron

Table 9. Calculated Relative Energies ΔE and Relevant Complexation Energies ΔE_{com} (kcal/mol) for δ-PA and 1,4-E Reaction Channels of the Reaction System B^- (= OH^-, F^-) + Z-1-methoxy-2-butene (**2b**)

	NL-P/DZP//Xα/DZP		NL-SCF/TZ2P//NL-SCF/TZ2P			
	OH^-		OH^-		F^-	
system	ΔE	ΔE_{com}	ΔE	ΔE_{com}	ΔE	ΔE_{com}
B^- + **2b**	0.0		0.0		0.0	
$[BH, (\mathbf{2b}\text{-}H^{\delta})^-]_{syn}$	−27.8	−13.2	−32.3	−12.7	−22.9	−24.1
$[BH, (\mathbf{2b}\text{-}H^{\delta})^-]_{anti}$	*a*	*a*	−33.2	−13.6	*a*	*a*
$BH + (\mathbf{2b}\text{-}H^{\delta})^-$	−14.6		−19.6		+1.2	
$BH + [C_4H_6, MeO^-]$	−19.8	−7.1	−17.7	−14.4	+3.1	−14.4
$BH + C_4H_6 + MeO^-$	−12.7		−3.3		+17.5	

[a] Not calculated.

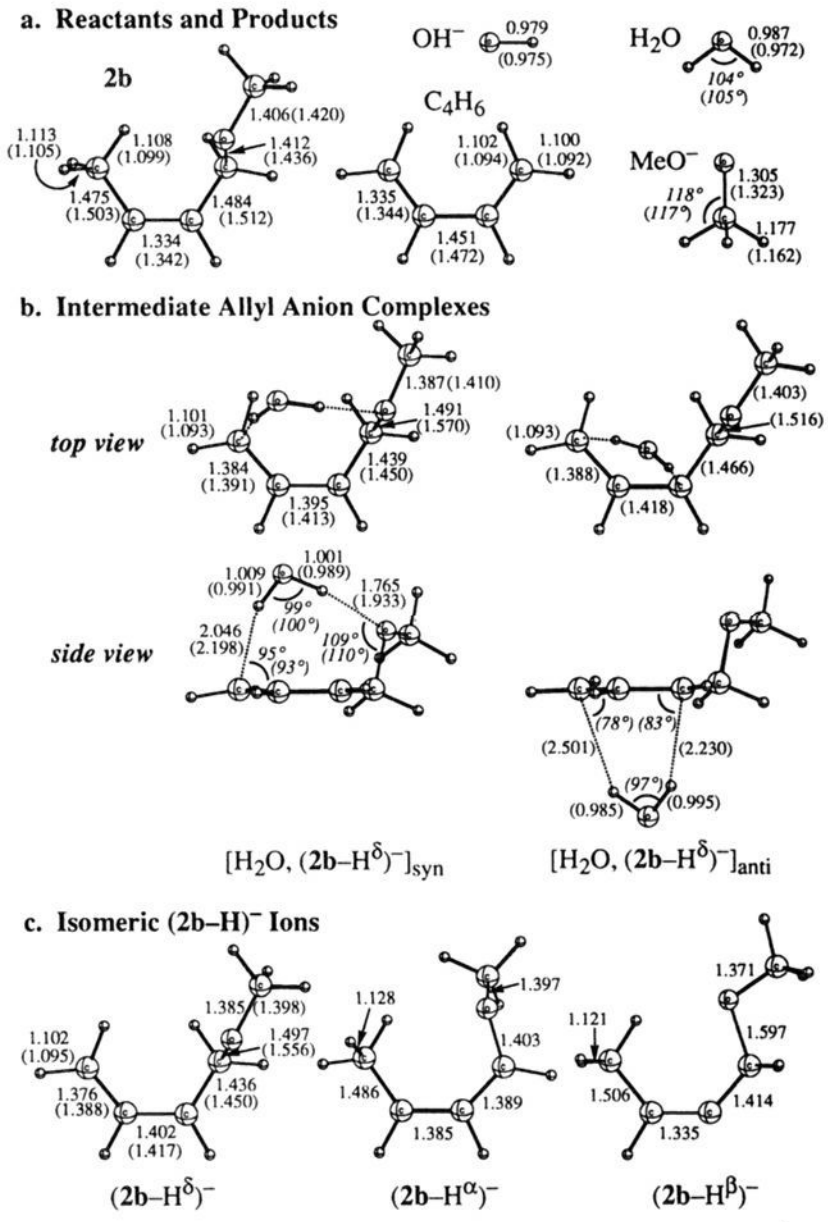

Figure 2. Selected Xα/DZP (and NL-SCF/TZ2P) structures (in Å and deg) on the OH^- + **2b** potential energy surface.

loss ($\Delta E_{EA^{vert}}$ = 14.1 kcal/mol) has increased relative to that of the prototype CH_2=CH-CH_2^- ($\Delta E_{EA^{vert}}$ = 3.3 kcal/mol), whereas $(\mathbf{2b}\text{-}H^{\alpha})^-$ has been destabilized ($\Delta E_{EA^{vert}}$ = 0.9 kcal/mol). The extremely low $\Delta E_{EA^{vert}}$ of $(\mathbf{2b}\text{-}H^{\alpha})^-$ is held responsible for facile thermal electron loss and, thus, its escape from mass spectrometric detection (see subsection B).

Nature of the 1,4-E Mechanism. Next, the nature of the mechanism of base-induced 1,4-eliminations is investigated in more detail through a scan of the 1,4-E potential energy surface of the OH^- and F^- + **2b** reaction systems. Optimized equilibrium structures and energies of the NL-P/DZP//Xα/DZP (for F: TZ2P) and NL-SCF/TZ2P//NL-SCF/TZ2P calculations are summarized in Figure 2 and Table 9. Generally, NL-SCF/TZ2P yields slightly shorter C−H and O−H bonds and longer C−C and C−O bonds than Xα/DZP. NL-SCF/TZ2P reaction energies for the 1,4-E elimination of OH^- and F^- + **2b** (−3.3 and +17.5 kcal/mol, Table 9) are within 4 kcal/mol of experimental ΔH_r values (+1 and +20 kcal/mol, Table 4). The corresponding NL-P/DZP//Xα/DZP result for OH^- + **2b** (−12.7 kcal/mol, Table 9) deviates more, i.e., by 14 kcal/mol. However,

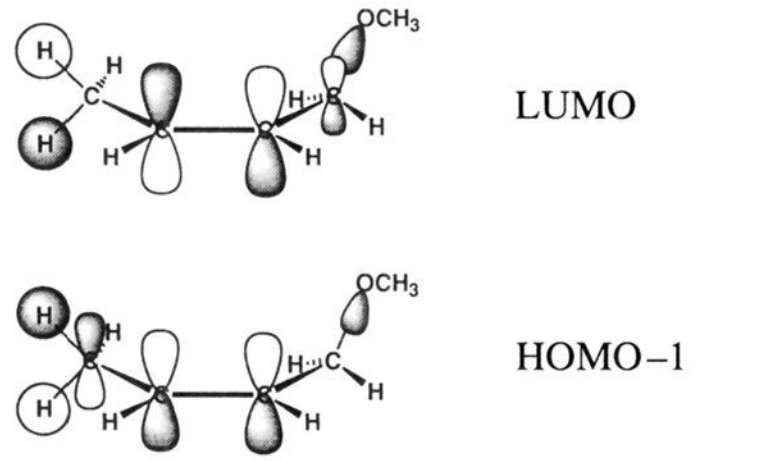

Figure 3. Schematic representation of the frontier orbitals of **2b**.

the main features of the OH^- + **2b** reaction profile are reproduced at both levels of theory. In the following, we discuss the higher level NL-SCF/TZ2P//NL-SCF/TZ2P results.

Association of OH^- and **2b** at H^{δ} may occur in a *syn* as well as in an *anti* fashion both leading to a barrierless proton transfer and the ca. −32 kcal/mol exothermic formation of a hydrogen bonded complex between water and the allyl anion, i.e., $[H_2O, (\mathbf{2b}\text{-}H^{\delta})^-]_{syn}$ and $[H_2O, (\mathbf{2b}\text{-}H^{\delta})^-]_{anti}$, which are bound by −12.7 and −13.6 kcal/mol, respectively (Table 9, Figure 2). In $[H_2O, (\mathbf{2b}\text{-}H^{\delta})^-]_{syn}$, one O−H bond ($d_{O-H}$ = 0.991 Å) of water points to C^{δ} (d_{C-H} = 2.198 Å) and the other one (d_{O-H} = 0.989 Å) to the oxygen of the methoxy group (d_{O-H} = 1.933 Å), thus building a cyclic structure with two (weak) hydrogen bonds (Figure 2). The C^{α}−OMe bond (d_{C-O} = 1.570 Å) has been elongated by ca. 0.1 Å with respect to **2b** (d_{C-O} = 1.436 Å), but it has not been broken. The formation of the allyl anion structure is accompanied by reduction and elongation of the $C^{\delta}-C^{\gamma}$ (d_{C-C} = 1.391 Å) and $C^{\gamma}-C^{\beta}$ bonds (d_{C-C} = 1.413 Å), respectively. The shortening of the $C^{\alpha}-C^{\beta}$ (d_{C-C} = 1.450 Å) reveals a slightly increased double bond character.

The base-induced structural changes of **2b** reflect directly the nature of its frontier orbitals (Figure 3). The **2b** LUMO is strongly anti-bonding across $C^{\beta}-C^{\gamma}$ and C^{α}−O and less so between H^{δ} and the C_4H_6 fragment. The HOMO is a lone-pair on oxygen. The HOMO-1 provides the $C^{\delta}-H^{\delta}$ σ as well as the $C^{\beta}-C^{\gamma}$ π bond, but it is anti-bonding across the $C^{\gamma}-C^{\delta}$ bond. During δ-proton transfer, the **2b** LUMO and HOMO-1 mix and transform into the unoccupied H^{δ} 1s orbital and the HOMO of the allyl anion (main amplitude on C^{δ} and C^{β}, node approximately on C^{γ}), respectively.

The structure of $[H_2O, (\mathbf{2b}\text{-}H^{\delta})^-]_{anti}$ is also cyclic but it differs from that of $[H_2O, (\mathbf{2b}\text{-}H^{\delta})^-]_{syn}$ in that both water O−H bonds point to an allylic carbon (C^{δ} and C^{β}). The (weak) water-leaving group hydrogen bond in $[H_2O, (\mathbf{2b}\text{-}H^{\delta})^-]_{syn}$ makes this complex predestined to react further via the 1,4-E_{solv} pathway leading to C_4H_6 + $[H_2O, MeO^-]$ (Scheme 2). In $(\mathbf{2b}\text{-}H^{\delta})^-$ the C−O bond (d_{C-O} = 1.556 Å) is again ca. 0.1 Å elongated with respect to **2b**, but it does not break. However, the leaving MeO^- group is only weakly bound by ca. −16 kcal/mol. This is in line with collision induced simple dissociation of the $(\mathbf{2}\text{-}H)^-$ ions (eq 11).

Scheme 4

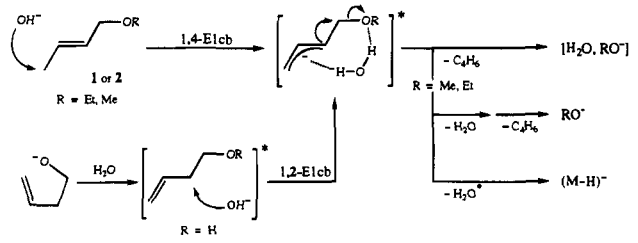

Alternatively, the allyl anion $(\mathbf{2b}\text{-}H^{\delta})^-$ may rearrange via an activation barrier of less than 16 kcal/mol to the ca. 2 kcal/mol less stable ion/molecule complex $[C_4H_6, MeO^-]$ (ΔE_{com} = −14.4 kcal/mol, Table 9) prior to dissociation. Similarly, F^- + **2b** may react via a barrierless δ-PT under the ca. −23 kcal/mol exothermic formation of the intermediate hydrogen bonded allyl anion complex $[FH, (\mathbf{2b}\text{-}H^{\delta})^-]_{syn}$ ($d_{C^{\delta}-H^{\delta}}$ = 1.336 Å, $d_{H^{\delta}-F}$ = 1.236 Å, $\angle C^{\delta}H^{\delta}F$ = 172°). This is ascribed to the efficient stabilization of the carbanion by the dipolar hydrogen fluoride (ΔE_{com} = −24.1 kcal/mol!).[29] Concluding, these data show that the gas-phase base-induced 1,4-eliminations of **2b** follow an E1cb mechanism.

4. Discussion

The Mechanism of Base-Induced 1,4-Eliminations. The combined experimental and theoretical results provide evidence for an E1cb mechanism for the gas-phase base-induced 1,4-eliminations of **1** and **2** in which barrierless δ-proton transfer leads to the formation of an intermediate ion/molecule complex between the $(M\text{-}H)^-$ allyl anion (M = **1**, **2**) and the conjugate acid (exemplified for the base OH^- in Scheme 4). Proceeding from this key intermediate, the conjugate acid (H_2O) can be transferred to the leaving group which, under loss of C_4H_6, leads to the production of the solvated leaving group $[H_2O, RO^-]$ (1,4-E_{solv}, Scheme 2). Alternatively, H_2O is evaporated from the rovibrationally excited ion/molecule complex. The resulting $(M\text{-}H)^-$ ion either dissociates into C_4H_6 and free RO^- if sufficient internal energy remains (1,4-E, Scheme 2), or it is preserved as a weakly bound species (δ-PT, Scheme 2). This is probably subjected to a dynamic equilibrium between the allyl anion structure and the ca. 2 kcal/mol less stable ion/molecule complex $[C_4H_6, RO^-]$ (Table 9).

It is interesting to note that recently an allyl anion/molecule complex of the type $[H_2O, (M-H)^-]$ has been invoked as a key intermediate in the mechanism for the abundant formation of $[H_2O, OH^-]$[6b,8c] in the reaction of but-3-ene-1-oxide with H_2O, which proceeds via an OH^- induced 1,2-E1cb elimination of but-3-ene-1-ol (Scheme 4).[6b] This provides an independent route to the same type of intermediate ion/molecule complex as in the OH^- induced 1,4-E1cb eliminations of **1** or **2** (Scheme 4). The observation, that both reactions are relatively fast, underlines the accelerating effect of allylic activation on both base-induced 1,2-E (cf. Bickelhaupt *et al.*[6b]) and 1,4-E eliminations (Tables 1−4), as has also been pointed out by Rabasco and Kass.[15b] However, we stress the principal difference between allylic activation in base-induced 1,2-E and 1,4-E eliminations. It can optionally be added in the former, but it is inherently contained in the latter.

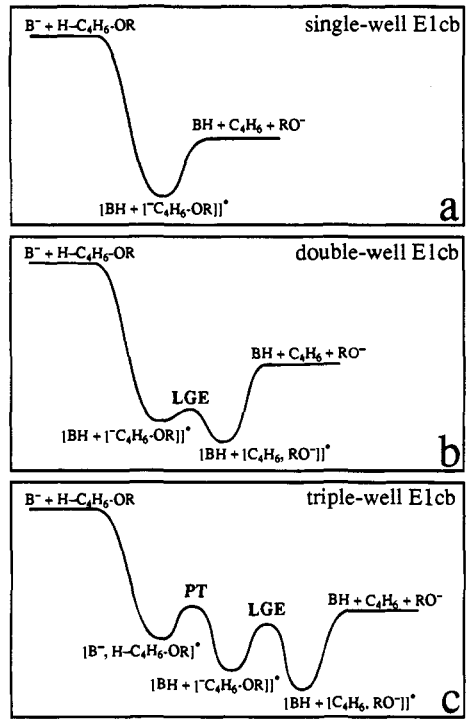

Figure 4. Schematic potential energy surfaces for gas-phase 1,4-E1cb mechanisms. (Transition states for proton transfer (PT) and leaving group expulsion (LGE) are indicated. For clarity, the increase in potential energy associated with eventual loss of BH from the intermediate complexes is omitted).

The theoretical results suggest that the E1cb mechanism of the base-induced 1,4-eliminations exists in various modifications. Three examples are presented for the 1,4-E pathway (Figure 4). In the first (Figure 4a), the reactants B^- + H-C_4H_6-OR combine via H^{δ} which leads to barrierless proton transfer (PT) and the formation of the intermediate ion/molecule complex [BH, $^-C_4H_6$-OR]*. Next, either before or after evaporation of BH, the leaving group expulsion (LGE) advances from [$^-C_4H_6$-OR]* without a reverse activation barrier. (For clarity, the increase in potential energy associated with the loss of BH is omitted in Figure 4!). This constitutes a single-well E1cb mechanism (Figure 4a) which has no counterpart in condensed-phase organic chemistry and which, to our knowledge, is unprecedented as a concept.[1-5,11] It is noted, however, that single-well mechanisms have also been proposed for the gas-phase addition−elimination reactions of strong nucleophiles (e.g., R_2N^- and RO^-) to the carbonyl carbon atom of amides and esters[18c] (see also ref 29). Alternatively (Figure 4b), the leaving group expulsion (LGE) from [$^-C_4H_6$-OR]* proceeds via rearrangement to an ion/molecule complex $[C_4H_6, RO^-]$*, prior to dissociation to the products. This is a double-well E1cb mechanism (Figure 4b) which corresponds to a (hypothetical) one-step E1cb mechanism in the condensed phase. Finally, it is also possible that the reactants collide such that B^- approaches H-C_4H_6-OR outside the H^{δ} reaction cone (Figure 4c). This leads to the formation of a stable reactant complex [B^-, H-C_4H_6-OR]*, from which proton transfer (PT) occurs. However, a (small) energy barrier is provided by the rearrangement which is required to bring the base in the appropriate orientation for protophilic attack (Figure 4c). This is in line with previous

(27) Dahlke, G. D.; Kass, S. R. *J. Am. Chem. Soc.* **1991**, *113*, 5566, and references cited therein.

(28) (a) Bickelhaupt, F. M.; de Koning, L. J.; Nibbering, N. M. M.; Baerends, E. J. *J. Phys. Org. Chem.* **1992**, *5*, 179. (b) Sheldon, J. C.; Currie, G. J.; Bowie, J. H. *J. Chem. Soc., Perkin Trans. 2* **1986**, 941.

(29) Scheiner and co-workers have already pointed out that strong and short hydrogen bonds yield low barriers or even single well potentials for proton transfer. See, for example: (a) Scheiner, S. *Acc. Chem. Res.* **1985**, *18*, 174. (b) Scheiner, S.; Latajka, Z. *J. Phys. Chem.* **1987**, *91*, 724.

(30) (a) Su, T.; Bowers, M. T. *Int. J. Mass Spectrom. Ion Phys.* **1975**, *17*, 211. (b) Su, T.; Bowers, M. T. *Int. J. Mass Spectrom. Ion Phys.* **1973**, *12*, 347. (c) Su, T.; Bowers, M. T. *J. Chem. Phys.* **1973**, *58*, 3027.

(31) Data used for the ADO calculations: μ_D(**2b**) = 0.899 D (NL-SCF/TZ2P//NL-SCF/TZ2P), α(**2**) = 10.539 Å^3 (calculated using data from ref 21c).

(32) van der Wel, H.; Bruin, G. J. M.; van der Linde, S. J. J.; Nibbering, N. M. M.; Engberts, J. B. F. N. *Recl. Trav. Chim. Pays-Bas* **1988**, *107*, 370.

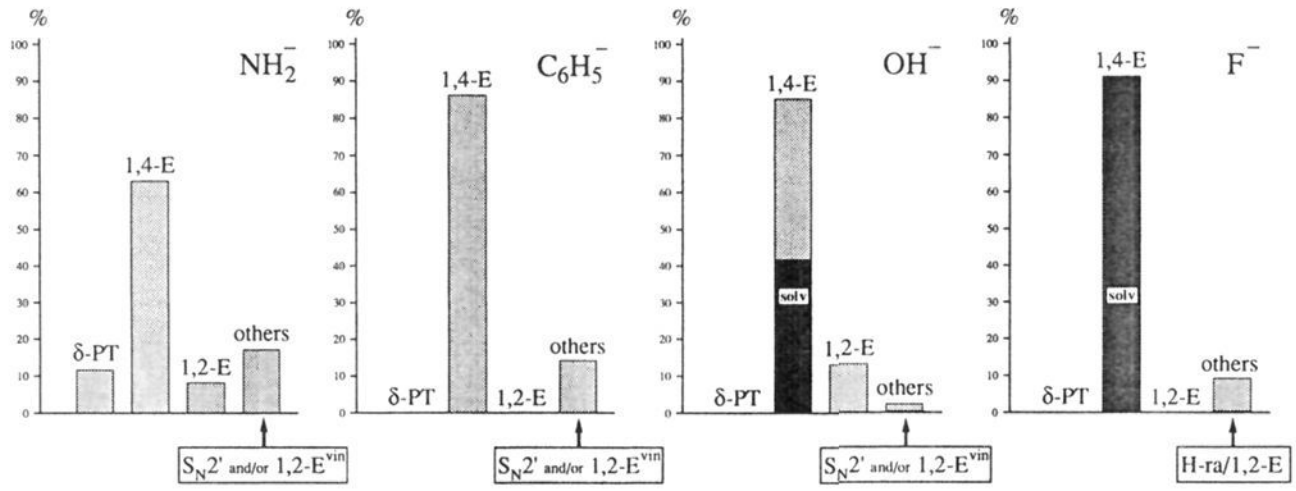

Figure 5. Estimated relative contribution of the various mechanisms (in %) in the reactions of **1** with NH_2^-, $C_6H_5^-$, OH^-, and F^-.

theoretical studies of anionic (NH_2^-, $ClCH_2^- + CH_3Cl$)[28a] and cationic ($CH_3OH + CH_3\text{-}OH_2^+$)[28b] S_N2 reactions, which show that the main source of the energy barrier originates from bringing the base in the right orientation for back-side nucleophilic attack on C^α. Together, these results demonstrate that orientation effects play a key role in gas-phase ion/molecule reactions. This constitutes a triple-well E1cb mechanism which closely resembles the well-known two-step E1cb elimination in the condensed phase[1] if the leaving group expulsion (LGE) also proceeds via a barrier (Figure 4c).

Reaction Rates and Competing Mechanisms. Base-induced reactions of **1** and **2** are extremely fast (Tables 1 and 3). Oxygen bases are the most reactive with a maximum bimolecular rate constant of 66×10^{-10} cm^3 molecule^{-1} s^{-1} for $OH^- + \mathbf{1}$, followed by the nitrogen bases with a maximum bimolecular rate constant of 41×10^{-10} cm^3 molecule^{-1} s^{-1} for $NH_2^- + \mathbf{1}$ (Table 1). Thus, some of our experimental rate constants exceed the average dipole orientation (ADO)[30] collision rate constant (e.g., $k_{ADO} = 24 \times 10^{-10}$ cm^3 molecule^{-1} s^{-1} for $OH^- + \mathbf{1}$).[31] Similar observations have been made before.[8c,21d,32] The reason for this is not clear. A tentative explanation might be a higher pressure of the substrates in the cell due to a larger pressure gradient than for the much lighter CH_4 used for the calibration of the ionization gauge manometer. The relative contributions of the competing mechanisms of four typical base-induced reactions, namely NH_2^-, $C_6H_5^-$, OH^-, and $F^- + \mathbf{1}$, are graphically displayed in Figure 5. The contribution of 1,4-E + 1,4-E_{solv} (Scheme 2) is ca 63, 86, 85, and 91%, respectively. Thus, the two pathways for 1,4-elimination represent by far the dominating mechanisms in all cases and are thus primarily responsible for the high reaction rates. The contribution of the 1,4-E_{solv} with respect to the 1,4-E mechanism increases when the proton affinity of the base decreases (Figure 5, Tables 1 and 3). This is explained by the fact that the energy released upon complexation between the conjugate acid and leaving group in the 1,4-E_{solv} mechanism becomes increasingly important to fuel the more and more endothermic reaction (Table 2). δ-Proton transfer (δ-PT) from **1** only occurs for NH_2^- (12%), amongst the four bases considered in Figure 5. This indicates that the conjugate acid NH_3 evaporates from the complex shortly after PT and, compared to other bases, efficiently carries away the released reaction exothermicity before randomization over the entire [NH_3, (**1**-H^δ)$^-$]* complex takes place. The base-induced 1,2-elimination (1,2-E, Scheme 2) is only observed for NH_2^- (8%) and OH^- (13%) where it contributes nearly an order of magnitude (7−8 times) less than the 1,4-elimination. The 1,2-E pathway of $F^- + \mathbf{1}$ is too endothermic (+19 kcal/mol, Table 2) to proceed under low-pressure conditions.[26] Instead, first an allylic hydrogen rearrangement transforms the leaving group but-2-ene-1-oxide into the more stable enolate anion but-1-ene-1-oxide; only then, F^- induced 1,2-elimination takes place (1,3-H-shift/1,2-E, eq 7). For the stronger bases, there is also a contribution from allylic nucleophilic substitution (S_N2') and/or vinylic 1,2-elimination (1,2-E^{vin}, Scheme 2). These pathways cannot be distinguished on the basis of the available experimental and thermochemical data. However, we suggest that 1,2-E^{vin} makes the major contribution. This is likely in the light of the general prevalence of the entropically more favorable elimination processes over substitutions in the gas phase. Furthermore, vinylic 1,2-elimination has been determined to make a 82% contribution in the NH_2^- induced reactions of the specifically deuterium labeled substrate 2,6,6-d_3-1-methoxy-4,4-dimethyl-1-vinyl-2-cyclohexene.[15b]

Finally, an interesting comparison can be made with the results of Rabasco and Kass[15c] for the base-induced reactions of **A** (eq 3) in which 1,4-elimination dominates for strong bases (NH_2^-, OH^-) but 1,2-elimination starts to compete successfully for weaker bases (MeO^-). These results apparently differ from our finding that 1,4-elimination generally dominates over 1,2-elimination in the base-induced reactions of the structurally closely related **1** (Figure 5, Table 1). The stronger tendency toward 1,4-elimination from **1** may be ascribed to the fact that this pathway is slightly (i.e., 2 kcal/mol) more exothermic than 1,2-elimination (Table 2), whereas both pathways yield the same products for **A**. Furthermore, the transition state of the base-induced 1,2-elimination from **A** is probably stabilized by a certain degree of interaction between the new α,β'- and the old β,γ-double bond. Such a kinetic assistance is absent in the base-induced 1,2-eliminations from **1**. Furthermore, our theoretical results suggest that the MeO^- induced 1,4-elimination from **A** may also proceed via an E1cb mechanism.

The Effect of *E*/*Z* Stereochemistry. The stereochemistry (i.e., *E* or *Z*) around the β,γ-double bond of the substrate has been found to have no detectable influence of the course of the base-induced 1,4-eliminations of **1** and **2**, e.g., the competition between 1,4-E and 1,4-E_{solv}. This is somewhat unexpected, because the *Z* stereoisomer seems to be more suitable for the formation of a [BH, RO^-] ion/molecule complex than the *E* stereoisomer due to the proximity of C^α and C^δ.[17] This is also indicated by the (weak) hydrogen bond between water and the methoxy oxygen in [H_2O, (**2b**-H^δ)$^-$]$_A$ (Figure 2). The observed independence of the 1,4-E versus 1,4-E_{solv} competition on the *E*/*Z* stereochemistry indicates that the energy barrier for the transfer of the conjugate acid BH from C^δ along the allyl anion system to the leaving group is essentially equal for the *E* and *Z* stereoisomers. We suggest that eventually the effect of the *E*/*Z* stereochemistry may become detectable when the internal energy of the rovibrationally excited intermediate [BH, (M-H^δ)]* is reduced through collisional cooling of the reactants (e.g., in the flow tube of a low temperature flowing afterglow apparatus[27]), because this causes a more critical dependence on small differences of the potential energy surfaces.

5. Conclusions

Base-induced 1,4-eliminations are extremely facile processes which compete effectively with simple proton transfer, 1,2-elimination, and vinylic 1,2-elimination as well as aliphatic (S_N2) and allylic (S_N2') substitution in the low-pressure gas-phase reactions of CH_3-CH=CH-CH_2-OEt (**1**). This follows from our FT-ICR study of the reactions of the allylic ethers **1**−**3** with a variety of anionic first-row bases. The fastest reactions take place with oxygen bases (e.g., OH^-) followed by the nitrogen bases (e.g., NH_2^-). The ionic products of base-induced 1,4-elimination are either the bare leaving group, RO^-, or the leaving group solvated by the conjugate acid of the base, [BH, RO^-]. The latter pathway becomes dominant for weaker bases (e.g., F^-), because the complexation energy compensates for the reduced exothermicity. This makes the reaction an efficient tool for the synthesis of solvated anions under low pressure conditions.

The stereochemistry (i.e., *E* or *Z*) around the β,γ-double bond of the substrate appears to have no detectable influence on the course of the base-induced 1,4-eliminations, probably because of relatively small differences on the corresponding potential energy surfaces.

The combined experimental and theoretical results provide evidence for an E1cb mechanism for the gas-phase base-induced 1,4-eliminations of **1** and **2** in which a complex between the $(M-H)^-$ allyl anion (M = **1**, **2**) and the conjugate acid is formed via a barrierless δ-proton transfer. This ion/molecule complex plays a key role as an intermediate from which the 1,4-E and 1,4-E_{solv} as well as δ-PT products are formed (Scheme 4).

The E1cb mechanism of the base-induced 1,4-eliminations exists in various modifications (Figure 5). It can proceed via a barrierless association and proton transfer (PT), followed by leaving group expulsion (LGE) without a reverse activation barrier (either before or after evaporation of BH). This constitutes a single-well E1cb mechanism (Figure 4a) which to our knowledge has no counterpart in condensed-phase organic chemistry[1-5,11] and is unprecedented as a concept. Alternatively, LGE proceeds via rearrangement to an ion/molecule complex prior to dissociation to the products, thus constituting a double-well E1cb mechanism (Figure 4b). Finally, B^- and H-C_4H_6-OR can form a stable reactant complex [B^-, H-C_4H_6-OR]* as long as they do not collide via H^δ. Next, PT advances via a (small) barrier which is associated with bringing the base in the right orientation for protophilic attack (Figure 4c). This constitutes a triple-well E1cb mechanism which closely resembles the well-known two-step E1cb elimination in the condensed phase[1] if LGE proceeds also via a barrier (Figure 4c).

Acknowledgment. This investigation was supported by the Netherlands Organization for Scientific Research (SON/NCF/NWO) and the Deutsche Forschungsgemeinschaft (DFG). We wish to thank Mrs. T. A. Molenaar-Langeveld for assistance with the syntheses. F.M.B. gratefully acknowledges a post-doctoral DFG fellowship.

JA950378A